Correspondence and requests for materials should be addressed to D.M. (davide.maggi@unige.it)

**Metformin Impairs Glucose Consumption and Survival in Calu-1 Cells by Direct Inhibition of Hexokinase-II.**

Barbara Salani[1,2*], Cecilia Marini[3*], Alberto Del Rio[4*], Silvia Ravera[5], Michela Massollo[2,6], Anna Maria Orengo[2], Adriana Amaro[2,7], Mario Passalacqua[8], Sara Maffioli[1,2], Ulrich Pfeffer[2,7], Renzo Cordera[1,2], Davide Maggi[1,2] and Gianmario Sambuceti[2,6].

[1]Department of Internal Medicine (DIMI) University of Genova, 16132, Genova, Italy; [2]IRCCS Azienda Ospedaliera Universitaria San Martino- IST Istituto Nazionale per la Ricerca sul Cancro, 16132, Genova, Italy; [3]CNR Institute of Molecular Bioimaging and Physiology (IBFM), Genova section, 16132, Genova, Italy; [4]Department of Experimental, Diagnostic and Specialty Medicine (DIMES), Alma Mater Studiorum–University of Bologna, 40126, Bologna, Italy; [5]Department of Pharmacy (DIFAR), University of Genova, 16132, Genova, Italy; [6]Nuclear Medicine, Department of Health Science (DISSAL), University of Genova, 16132, Genova, Italy; [7]Italian Institute of Biostructures and Biosystems (INBB), University of Genova, 16132, Genova, Italy; [8]Department of Experimental Medicine (DIMES), University of Genova, 16132, Genova, Italy.
* These authors contributed equally to this work

**Supplemental Figures**
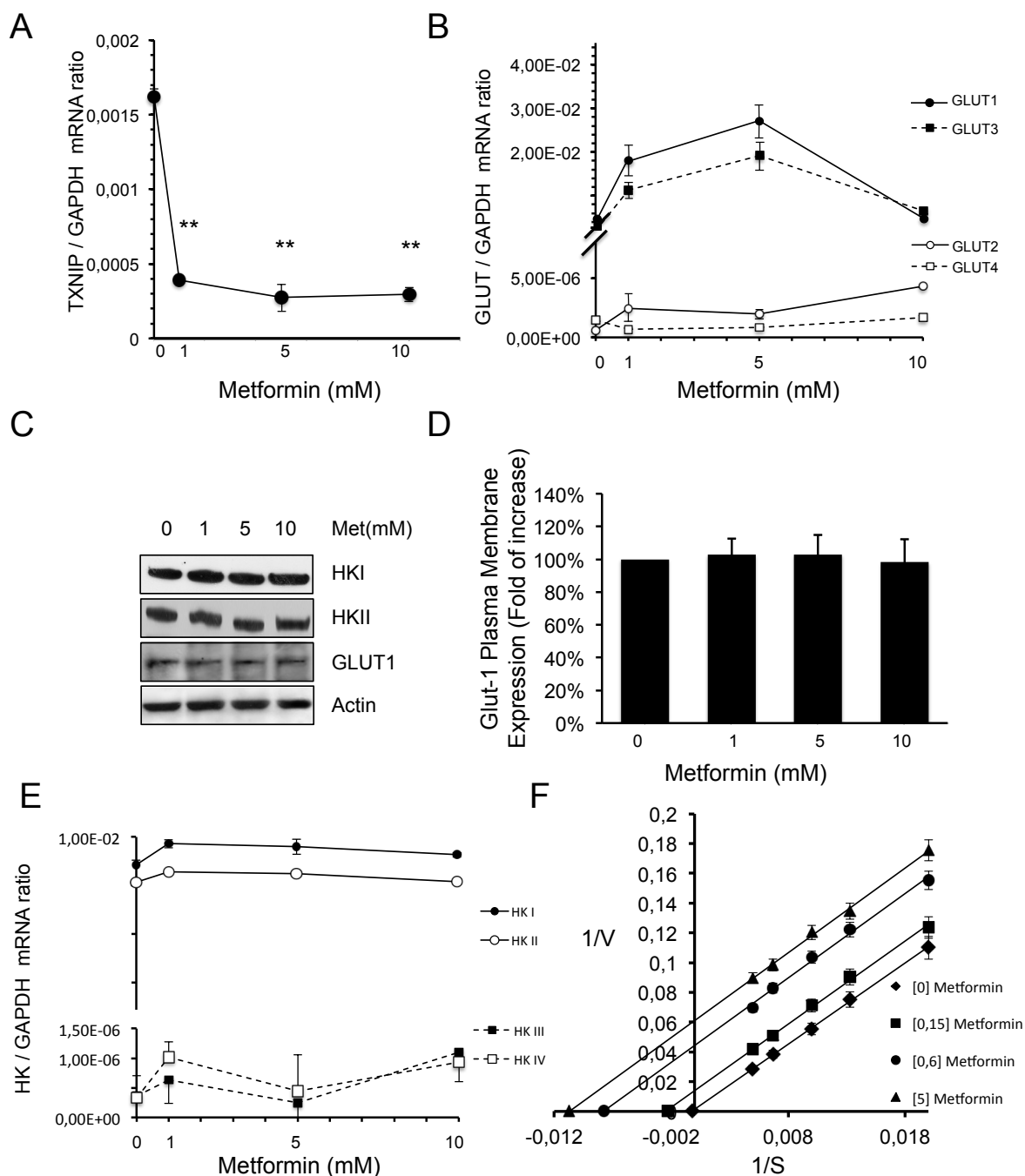


**Figure S1.** Metformin effect on AMPK phosphorylation and TXNIP and GLUTs expression following 24hr of metformin treatment in Calu-1 cells. (A) RT–PCR analysis of TXNIP. (B) RT–PCR analysis of GLUT1-4. (C) Western blot analysis of Calu-1 total cell lysates probed with specific antibodies for HKI, HKII, GLUT1 and Actin. (D) Plasma membrane GLUT1 expression. (E) RT–PCR analysis of HKI-II-III-IV. (F) Lineweaver-Burk plot of the human purified HKII activity, in the presence of different concentration of glucose and metformin.
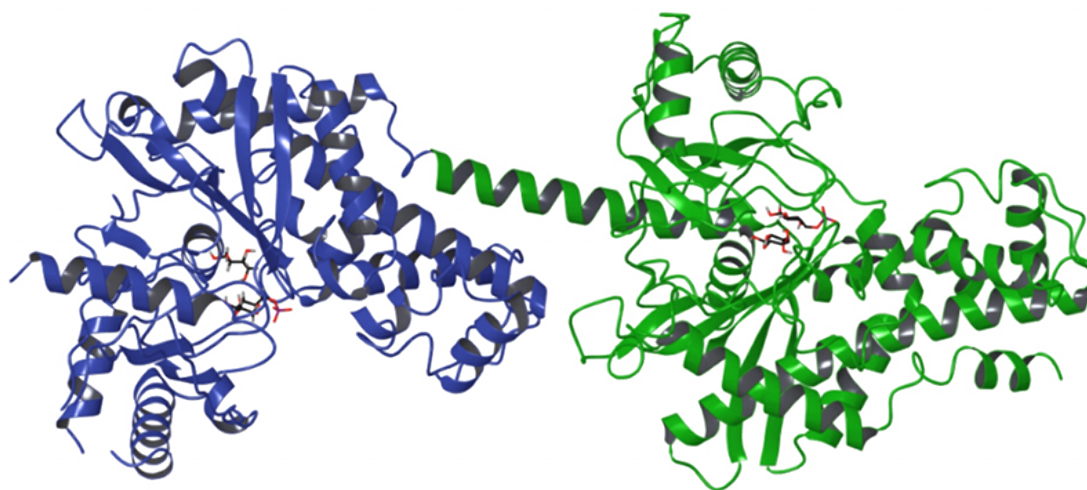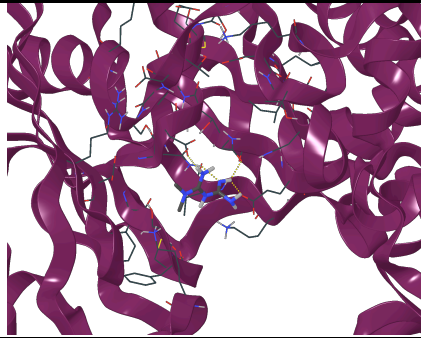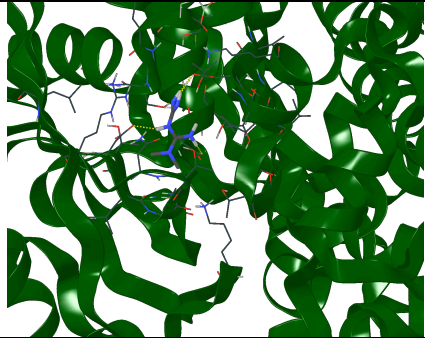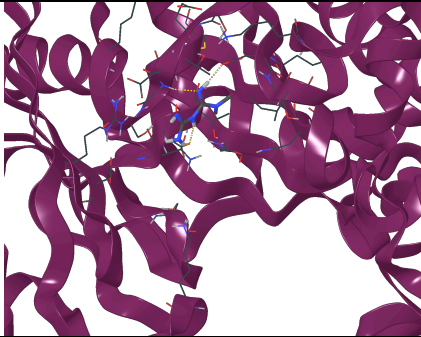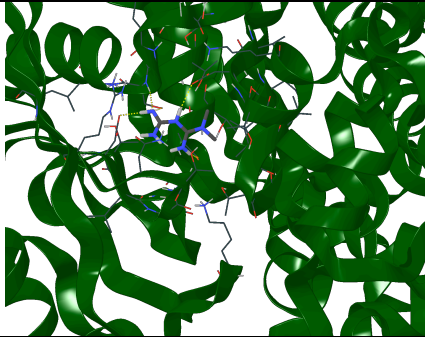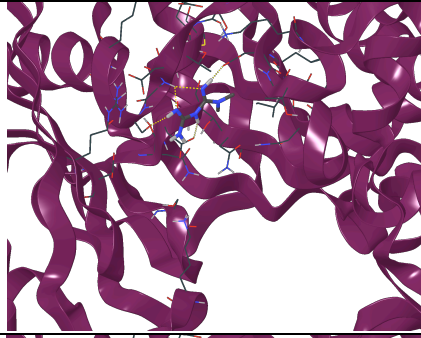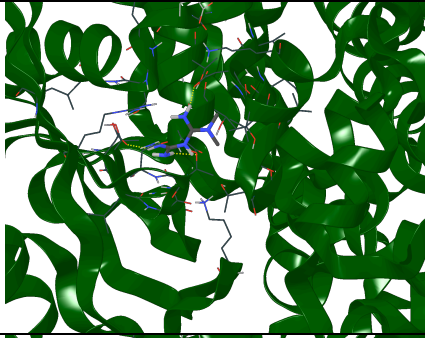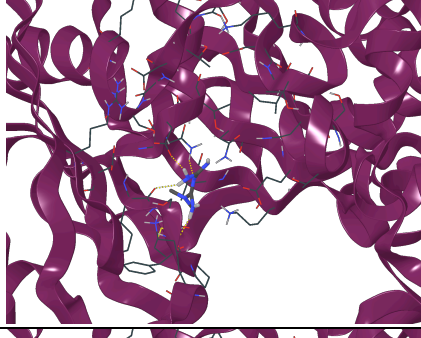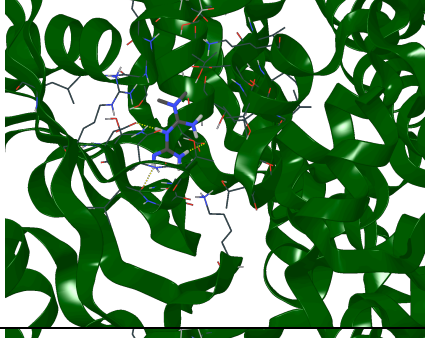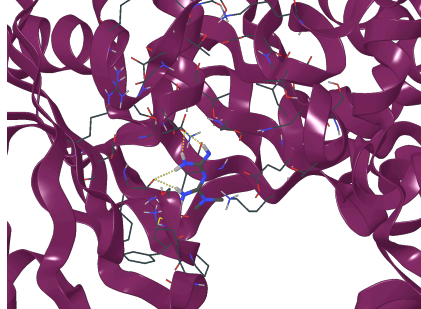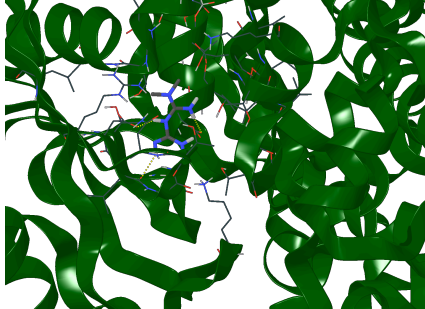
**Figure S2 (Related to Figure 2)**. Stucture of the Hexokinase II in complex with glucose-6-phosphate and glucose (PDB code 2NZT). The blue ribbon shows the C-terminal catalytic domain while the green the N-terminal regulatory domain. The catalytic domain was used to perform all *in silico* calculations.
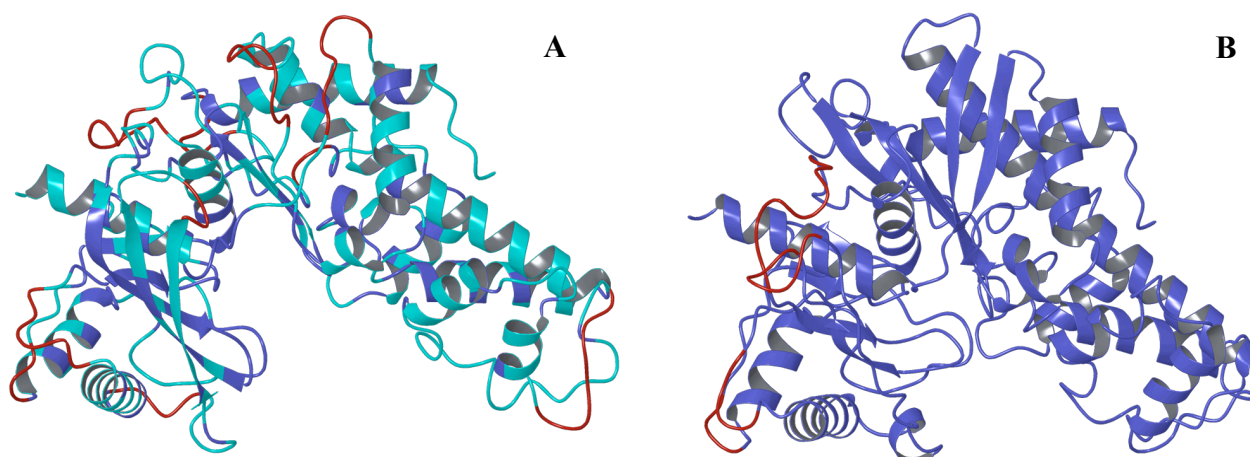


**Figure S3 (Related to Figure 2).** Ribbon representation of the homology model resulting for the open form (A) and the closed form (B). Conformation of blue residues was copied from template crystallographic structures as they represent identical residues. Cyan residues represent those where the backbone conformation is copied from template crystallographic structures but side-chain mutations were modeled consistently to mutations at this position in the human HKII sequence. Red residues were modeled in both backbone and sidechains as no structural data are available in these regions. None of the reconstructed loops is in proximity of the catalytic site.
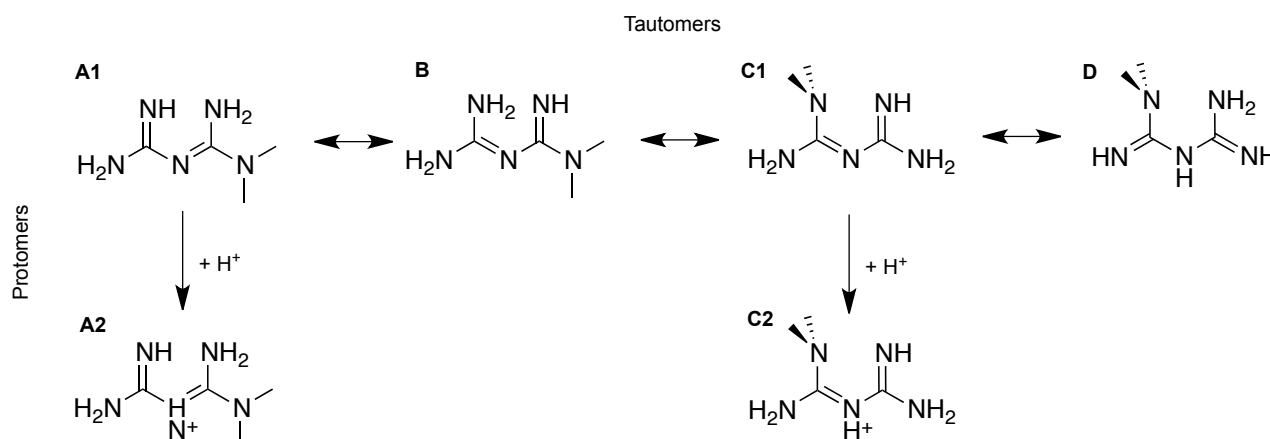


**Figure S4 (Related to Figure 2).** Stable tautomeric and protonation forms of metformin. Tautomers (A1, B, C1 and D) represent those that are considered to be the more stable[1,2]. Protonation states of these tautomers were calculated with EPIK software (Version 2.3.023) by retaining all possible combination in the pH range of 7.0 ± 2.0. As a result, protomers A2 and C2 were generated.

| Pose number | Open conformation | Closed conformation |
|:---:|:---:|:---:|
| 1 |  |  |
| 2 |  |  |
| 3 |  |  |
| 4 |  |  |
| 5 |  |  |

**Figure S5 (Related to Figure 2)**. Representative binding modes of metformin as listed in Table S4. In the open conformation metformin show multiple binding locations with poor docking score. On the other hand, in the closed conformation metformin bind to a specific region (the glucose-6-phosphate binding site) with high docking score.
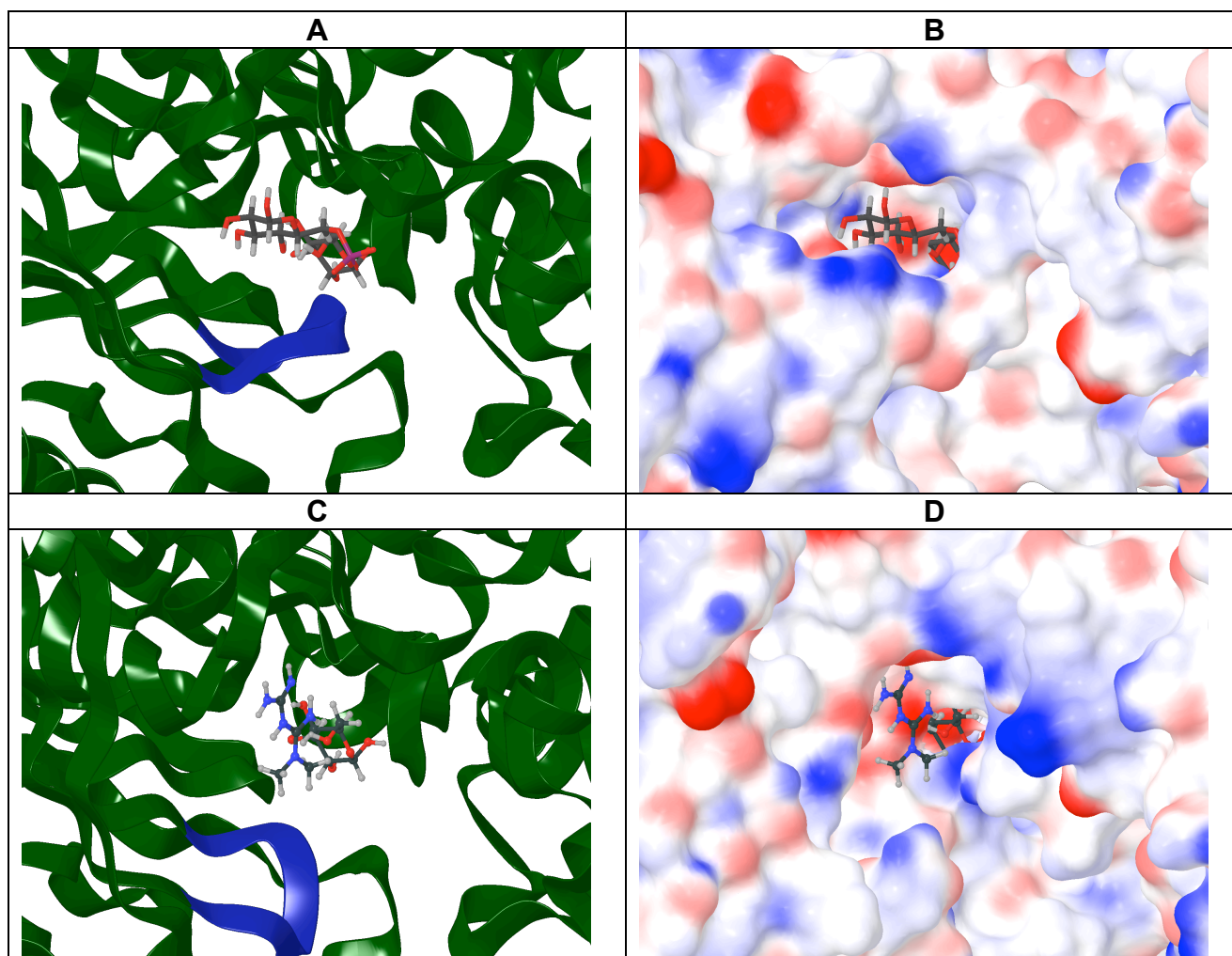
**Figure S6 (Related to Figure 2)**.(A) Ribbon representation and, (B) molecular surface of the crystallographic structure of HKII in the closed conformation (PDB ID: 2NTZ). (C) Ribbon representation and, (D) molecular surface obtained after 25ns molecular dynamic simulations of the closed HKII in complex with metformin and glucose. The metformin binding essentially unaffected the conformation of the inner catalytic site suggesting that it can be conveniently used for the rational design of other small-molecule inhibitors of HKII[3,4]. Of note, is the only movement of the external loop (in blue, A and C) that opens up in the case of metformin binding (C) while is closed with glucose-6-phosphate binding (A).

## Supplemental Tables

**Table S1**. List of structural templates used to build the homology model of the open form of HKII

| Protein | Organism | PDB ID | Resolution [Å] | Chain[b] | Used to reconstruct[a] |
|---|---|---|---|---|---|
| Hexokinase II | *Saccharomyces cerevisiae* | 1IG8[5] | 2.20 | A (1-486) | 476-917 |
| Hexokinase | *Sulfolobus tokodaii* | 2E2P[6] | 2.00 | A (1-299) | ADP[c] |

a)      Human HK2 numbering
b)      Protein Data Bank chain numbering
c)      ADP was manually modified to ATP

**Table S2**. List of structural templates used to build the homology model of the closed form of HKII binding with glucose and its endogenous inhibitor glucose-6-phosphate.

| Protein | Organism | PDB ID | Resolution [Å] | Chain[b] | Used to reconstruct[a] |
|---|---|---|---|---|---|
| Hexokinase II | *Homo Sapiens* | 2NZT[7] | 2.20 | A (476-913) | 476-917, GLC and BG6 |

a)      Human HK2 numbering
b)      Protein Data Bank chain numbering

**Table S3**. List of structural templates used to build the homology model of the closed form of HKII in its active form binding with ATP, glucose and the $Mg^{2+}$ ion.

| Protein (Uniprot ID) | Organism | PDB ID | Resolution [Å] | Chain[b] | Used to reconstruct[a] |
|---|---|---|---|---|---|
| Hexokinase II | *Homo Sapiens* | 2NZT[7] | 2.20 | A (476-913) | 476-779, 787-917 and GLC |
| Hexokinase I | *Homo Sapiens* | 1DGK[8] | 2.80 | A (476-913) | 780-786 |
| Hexokinase | *Sulfolobus tokodaii* | 2E2Q[6] | 2.00 | A (1-297) | $Mg^{2+}$ and ADP[c] |

a)      Human HK2 numbering
b)      Protein Data Bank chain numbering
c)      ADP was manually modified to ATP

**Table S4**. List of the five most stable binding poses of metformin in the open and closed HKII conformations obtained with induced fit docking calculations. Results are sorted by docking score (XP score) as calculated by Glide software (Version 5.8.023). The open conformation cannot accommodate metformin with a stable binding mode while the closed conformation can steadily harbor different orientation of metformin (see also Figure S4).

| Pose number | Open conformation | | Closed conformation | |
|---|---|---|---|---|
| | *Metformin form[a]* | *Induced fit docking score* | *Metformin form[a]* | *Induced fit docking score* |
| 1 | A2 | -3.485 | A2 | -4.762 |
| 2 | D | -3.444 | A2 | -4.365 |
| 3 | D | -3.423 | A2 | -4.470 |
| 4 | A1 | -3.350 | A2 | -4.498 |
| 5 | A1 | -3.317 | A2 | -4.034 |

a)      Names reported in supplementary material Figure S2.

# Movie legends

**Media video 1**. Molecular dynamic trajectory of 25ns simulation of the most stable binding pose of metformin in the closed HKII conformation (see pose 1, Table 4 and Figure 4, supplementary material).

**Media video 2**. Molecular dynamic trajectory of 25ns simulation of the second most stable binding pose of metformin in the closed HKII conformation (see pose 2, Table 4 and Figure 4, supplementary material).

# Supplemental Methods

### Models of Hexokinase II
Two models of the catalytic domain of Hexokinase II were generated and used in this study (Figure S2). The open form is characteristic of hexokinase without substrate (Figure 2a). The closed form is characteristic of hexokinase conformation induced upon glucose binding. The closed conformation accommodate glucose, ATP and either a magnesium ion to catalyze the phosphorylation reaction (Fig. 2d) or the glucose-6-phosphate that auto-inhibit the catalytic activity of HKII.

The primary sequence of the catalytic domain of human Hexokinase II was obtained in FASTA from the Uniprot database (ID: P52789[476-913]) as a query sequence. Homology modeling of the open and closed forms was obtained by using various crystallographic templates available from the Protein Data Bank (Table S1, S2 and S3). Structural data were processed with common preparation routines that included: assignment of bond orders, addition of hydrogens, creation of zero-order bond to $Mg^{2+}$, sampling water orientation and optimization of Asn, Gln and His residue protonation states. These routines were performed with Maestro version 9.3.023.

Homology composite models were constructed by using the template structures reported below by applying the following settings: i) alignment of structure with *multiple alignment* tool (Prime software) and *protein structure alignment* tool (Maestro), ii) knowledge-based mode algorithm, iii) retention of rotamers for conserved residues, iv) optimization of side chains, and v) building of insertions of up to 20 residues.

The homology models were minimized with the *restrained minimization* routine of the *protein preparation wizard* tool by converging heavy atoms to an RMSD of 0.30Å. Some protein loops located far from the binding sites of ATP, glucose, $Mg^{2+}$, glucose-6-phosphate and metformin were reconstructed with Prime software (Figure S2). Prime software version 3.1.023 and Maestro version 9.3.023 were used to obtain and refine the initial homology models. Calculations were carried out on a Linux x86_64 platform machine equipped with an Intel Core2 Quad CPU (Q9400, 2.66GHz).

Molecular dynamic simulations (MD) were carried out on homology models of the open and closed forms HKII to assess the stability of these conformations. A multistep *relaxation protocol*, that included a series of minimizations and short molecular dynamics simulations, was performed to relax the homology model systems. In particular, the following steps were performed:

- Step 1. Build of the model system with: SPC solvent, boundary conditions with orthorhombic box shape, box size calculated with buffer method and, neutralization of the model system with variable number of $Na^+$ ions.
- Step 2. Minimization with the solute restrained with a convergence threshold of 50.0 kcal/mol/Å
- Step 3. Minimization without restraints with a convergence threshold of 5.0 kcal/mol/Å
- Step 4. Simulation in the NVT ensemble using a Berendsen thermostat with: simulation time of 12ps; temperature of 10K; fast temperature relaxation constant; velocity resampling every 1ps and non-hydrogen solute atoms restrained
- Step 5. Simulation in the NPT ensemble using a Berendsen thermostat and a Berendsen barostat with: simulation time of 12ps; temperature of 10K, pressure of 1 atm; fast temperature relaxation constant; slow pressure relaxation constant; velocity resampling every 1ps and non-hydrogen solute atoms restrained

- Step 6. Simulation in the NPT ensemble using a Berendsen thermostat and a Berendsen barostat with: simulation time of 24ps, temperature of 300K, pressure of 1 atm, fast temperature relaxation constant, slow pressure relaxation constant, velocity resampling every 1ps and non-hydrogen solute atoms restrained
- Step 7. Simulation in the NPT ensemble using a Berendsen thermostat and a Berendsen barostat with: simulation time of 24ps, temperature of 300K, pressure of 1 atm, fast temperature relaxation constant, normal pressure relaxation constant and no restraints.

These steps were followed by a 1.2ns simulation in the NPT ensemble using: a MTK thermostat and a MTK barostat, temperature of 300K, pressure of 1 atm, normal pressure relaxation constant and no restraints. These simulations confirmed the binding modes of glucose, glucose-6-phosphate, ATP and $Mg^{2+}$ in the two homology models (Figures 2a, 2b, 2c and 2d). The ATP showed the ability to bind both the open and the closed HKII conformation (Figures 2a and 2d) consistently to previous crystallographic experiments. The last MD snapshot of each model was further minimized without restraints by using the *minimization* routine of the *Desmond* program with a convergence threshold of 1.0 kcal/mol/Å and were used as input geometry for molecular docking simulations.

All MD simulations (including those described below) were performed with Desmond molecular dynamics system software (Version 3.1.023) as implemented in the Schrodinger suite 9.3 update 1. Simulations were run on a Linux HPC equipped with Quad-Core AMD Opteron 2378 processors using a variable number of CPU cores per job.

## Molecular docking on Hexokinase II models

Hexokinase isoforms are known to undergo large conformational changes upon substrate binding[5]. Because of this flexibility we performed induced fit docking (IFD) calculations on metformin to assess the putative binding modes in the open and closed conformation of HKII.

Metformin in its different tautomeric and protonated states (Figure S3) was docked in the open and closed models of HKII. Induced fit docking were carried out with the following settings:

i) Exclusion of ATP, glucose, glucose-6-phosphate, $Mg^{2+}$ ion and water molecules in the receptor grids
ii) Enclosing box of 20Å-size centered on the catalytic residue of Asp657
iii) Flexible sampling of metformin (allow nitrogen inversion)
iv) Inclusion of up to 20 metformin poses per protomer and per tautomer
v) Refinement of residues within 5.0Å from the metformin poses (including side chains)
vi) Re-docking of structure within 30.0 kcal/mol of the best structure and within the top 20 structures overall
vii) Write out a maximum 3 poses per metformin protomer and tautomer
viii) *Extra precision* (XP) algorithm.

The best docking pose for both simulation was stored (Table S4) and visually inspected. Metformin poses in the closed HKII conformation were sensibly more stable that those of the open conformation. Docking simulations were performed with Glide software (Version 5.8.023) on a Linux x86_64 platform machine equipped with an Intel Core2 Quad CPU (Q9400, 2.66GHz).

Further investigations with molecular dynamic simulations were performed on the two most stable metformin poses in the closed HKII. Two simulations of 25.0ns each were carried out in the NPT ensemble using a MTK thermostat and a MTK barostat, temperature of 300K, pressure of 1 atm, normal pressure relaxation constant and a recording interval of energy each 10ps and trajectory recorded each 25ps. The analysis of MD trajectories confirmed the stability of the metformin binding modes obtained (Media video 1 and 2, supplementary information).

## Lineweaver-Burk plot of the human purified HKII.

HKII was incubated for 10' in a solution containing $MgCl_2$ (5 mM) and different concentrations of metformin (0 mM, 0,15 mM, 0,6 mM 5 mM) and glucose (50 mM, 75 mM, 100 mM, 150 mM, 200 mM). After ten minutes pre-incubation, the reaction was started providing ATP (0,8 mM). The straight lines appear parallel because both the Vmax and the Km decrease by the same factor indicating that metformin inhibition on HK activity is uncompetitive.

# Supplemental references

1) Sundriyal, S., Khanna, S., Saha, R. and Bharatam, P. V. Metformin and glitazones: does similarity in biomolecular mechanism originate from tautomerism in these drugs?. *J Phys Org Chem*. **21**, 30–33. (2008).

2) Bharatam, P. V, Patel, D. S. & Iqbal, P. Pharmacophoric features of biguanide derivatives: an electronic and structural analysis. *J Med Chem*. **48**, 7615–22. (2005).

3) Barbosa, A.J.M. & Del Rio, A. Freely accessible databases of commercial compounds for high-throughput virtual screenings. *Curr Top Med Chem*. **12**, 866–77. (2012).

4) Caporuscio, F., Rastelli, G., Imbriano, C. and Del Rio, A. Structure-based design of potent aromatase inhibitors by high-throughput docking. *J Med Chem*. **54**, 4006–17. (2011).

5) Kuser, P. R., Krauchenco, S., Antunes, O., Polikarpov, I. The high resolution crystal structure of yeast hexokinase PII with the correct primary sequence provides new insights into its mechanism of action. . *J Biol Chem.* **275**, 20814–21. (2000).

6) Nishimasu, H., Fushinobu, S., Shoun, H., Wakagi, T. Crystal structures of an ATP dependent hexokinase with broad substrate specificity from the hyperthermophilic archaeon Sulfolobus tokodaii. *J Biol Chem*. **282**, 9923–31. (2007).

7) Structural Genomic Consortium (SGC).

8) Aleshin, A.E. et al. Crystal structures of mutant monomeric hexokinase I reveal multiple ADP binding sites and conformational changes relevant to allosteric regulation. *J Mol Biol*. **296**, 1001–15. (2000)